The role of surface rheology in liquid film formation

2010 EPL 90 24002

(http://iopscience.iop.org/0295-5075/90/2/24002)

A Letters Journal Exploring the Frontiers of Physics

April 2010

EPL, **90** (2010) 24002 www.epljournal.org
doi: 10.1209/0295-5075/90/24002

The role of surface rheology in liquid film formation

B. Scheid[1,2(a)], J. Delacotte[3], B. Dollet[4], E. Rio[3], F. Restagno[3], E. A. van Nierop[1], I. Cantat[4], D. Langevin[3] and H. A. Stone[1,5]

[1] *School of Engineering and Applied Sciences, Harvard University - Cambridge, MA 02138, USA*
[2] *TIPs - Fluid Physics unit, Université Libre de Bruxelles - C.P. 165/67, 1050 Brussels, Belgium, EU*
[3] *Laboratoire de Physique des Solides UMR8502, Université Paris-Sud - 91405 Orsay, France, EU*
[4] *Institut de Physique de Rennes UMR6251, Université de Rennes - 35042 Rennes, France, EU*
[5] *Department of Mechanical and Aerospace Engineering, Princeton University - Princeton, NJ 08544, USA*

received 26 March 2010; accepted 19 April 2010
published online 6 May 2010

PACS 47.15.gm – Thin film flows
PACS 47.85.mb – Coating flows
PACS 68.03.-g – Gas-liquid and vacuum-liquid interfaces

Abstract – The role of surface rheology in fundamental fluid dynamical systems, such as liquid coating flows and soap film formation, is poorly understood. We investigate the role of surface viscosity in the classical film-coating problem. We propose a theoretical model that predicts film thickening based on a purely surface-viscous theory. The theory is supported by a set of new experimental data that demonstrates slight thickening even at very high surfactant concentrations for which Marangoni effects are irrelevant. The model and experiments represent a new regime that has not been identified before.

Introduction. – Although the concepts of surface viscosity and elasticity date back to Plateau in the 19th century, they have only recently been formalized mathematically and subsequently been used in quantitative descriptions of surface flows (see [1] for a historic review). The concepts of surface viscosity and elasticity (Marangoni) effects are intimately related, and are not always distinguishable in an experimental setting. Even in some of the simplest situations, there is debate over the role of surface rheology. One such configuration is the Landau-Levich-Derjaguin (LLD) dip-coating flow, wherein a film of wetting liquid is "deposited" onto a solid substrate as it is withdrawn from a bath. This process is so fundamental to coating flows that it is ubiquitous in today's coating technologies. The aim is always to deposit a film with a desired thickness, which is achieved by controlling the substrate withdrawal speed and the (bulk and surface) rheology of the liquid. The film thickness h_0 in a dip-coating process at speed u_0 usually follows the LLD-like law,

$$\frac{h_0}{\ell_c} = 0.9458\,\alpha\,Ca^{2/3}, \qquad (1)$$

where $\ell_c = \sqrt{\gamma/(\rho g)}$ is the capillary length and $Ca = \mu u_0/\gamma$ the capillary number, with μ the dynamic viscosity, ρ the density, γ the surface tension, and g the gravitational acceleration. Here α is a thickening factor that is tied to surface rheology and is a maximum of $4^{2/3}$ for immobile interfaces (in the frame of the film) [2].

There are open questions for flows where Marangoni effects are weak or are not expected to play a role. In particular, it is commonly assumed that, as for pure liquids, there is no thickening (*i.e.*, $\alpha = 1$) for liquids containing large amounts of soluble surfactants, such that the substrate withdrawal does not induce Marangoni stresses. However, in some cases thickening does occur (*e.g.*, [3]), again raising the prospect of a role for surface rheology. In this letter we show experimentally and theoretically that thickening in the absence of Marangoni effects can be explained by surface viscosity. Our work has relevance for dip-coating flows, as well as soap films formation and other flows involving fluid-fluid interfaces with surface-active materials. We first discuss the role of surfactant concentration on surface rheology, followed by the development of our model and a discussion of its results as compared to new experimental data.

Role of surfactant concentration. – At high surfactant concentration, exchanges between surface and volume are fast and can suppress the Marangoni effect that is caused by surface elasticity, thus rendering the interface

(a) E-mail: bscheid@ulb.ac.be

more mobile. This phenomenon, referred to as "surface remobilization" [4], requires two conditions to occur that are both fostered at high bulk surfactant concentration. First, the surfactant exchange rate between the interface and the sublayer has to be fast in comparison to the dilatation/compression rate of the interface, *e.g.*, [5] gives the dependence of surface elasticity with the rate of compression. Second, the film should be thick enough such that it contains enough surfactants to replenish the interface. Sonin *et al.* [6] showed that the drainage of very thin films is controlled by Marangoni effects and proceeds as if the surfactants were insoluble, even at high bulk concentration. This phenomenon was predicted earlier by Lucassen-Reynders and Lucassen [7], who proposed expressions for the decrease of the effective film elastic modulus with increasing film thickness.

In their study of fiber coating, Quéré and de Ryck [3] defined a parameter $\sigma = \Gamma/(c\,h_0)$, which measures the capacity of the "bulk reservoir" to replenish the interface with surfactant, where Γ is the surface concentration and c the bulk concentration. Using the soluble surfactant DTAB (dodecyl trimethyl ammonium bromide) at high concentration $c = 5\,\mathrm{cmc}$ ($\mathrm{cmc} = 15\,\mathrm{mM}$), they identified a "dynamical transition of thickening" by increasing the substrate speed (*i.e.* Ca), hence the film thickness, separating a region of large thickening ($\alpha \simeq 1.9$) before the transition, corresponding to $\sigma > 0.1$, from a region of small thickening ($\alpha \simeq 1.15$) beyond the transition, corresponding to $\sigma < 0.01$. This transition was shifted toward smaller Ca when increasing the concentration to $c = 25\,\mathrm{cmc}$ (see fig. 61 in [3]). For both concentrations used by these authors, the thickening factor beyond the transition remained unexpectedly larger than unity, and the thickening mechanism for such thicker films has not been explained as of yet. As mentioned earlier, surface elasticity, responsible for thickening at lower Ca, should not play a significant role after the transition because of surface remobilization. We demonstrate here that thickening beyond the transition can instead be rationalized by surface-viscous effects.

Model. – Consider a flat plate that is withdrawn from a bath of liquid and entrains a film of thickness $h(x)$ that eventually approaches a constant value h_0 at distances far above the static meniscus, as sketched in fig. 1. For a pure Newtonian fluid, this thickness is given by (1) with $\alpha = 1$ and the region that connects the static meniscus with the flat film, called the dynamic meniscus, has a typical length of $\ell_{Ca} = h_0\,Ca^{-1/3}$. Here we investigate how the thickening factor α is affected by surface viscosity, denoted $\mu*$. As in the usual LLD problem the film is thin enough in the dynamic meniscus region such that lubrication theory applies, *i.e.* $h_0/\ell \ll 1$. We further neglect gravity in the dynamic meniscus as compared to viscous stress, *i.e.* $\rho g \ll \mu u_0/h_0^2$. Under these assumptions, the velocity profile tends toward a uniform flow as $x \to \infty$ and the pressure relative to the ambient pressure remains constant across the film, *i.e.* $p = -\gamma \partial_{xx} h$. The axial-force balance

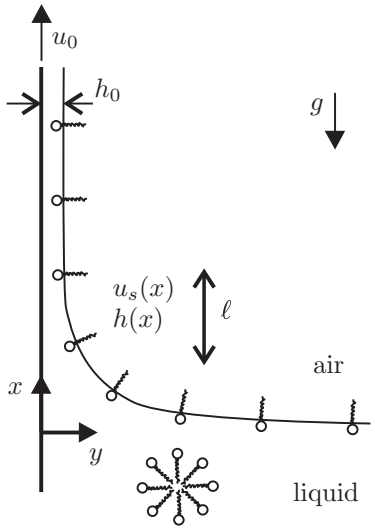

Fig. 1: Sketch of the dip-coating problem with surfactants at high concentration; $h(x)$ is the film thickness and $u_s(x)$ the surface velocity in the dynamic meniscus of length ℓ.

has the form

$$\mu \partial_{yy} u + \gamma \partial_{xxx} h = 0. \tag{2}$$

The axial velocity $u(x, y)$ is therefore parabolic in y and using $u|_{y=0} = u_0$, $u|_{y=h} = u_s(x)$ and $\int_0^h u(x, y)\,\mathrm{d}y = h_0 u_0$, the velocity in the film can be expressed as

$$\frac{u}{u_0} = 1 - \left(1 - \frac{u_s}{u_0}\right)\frac{y}{h} - 3\left(\frac{h - 2h_0}{h} + \frac{u_s}{u_0}\right)\frac{y}{h}\left(1 - \frac{y}{h}\right), \tag{3}$$

where $u_s(x)$ is the unknown surface velocity. The system is closed by the tangential stress balance at the interface (see, *e.g.*, [8]):

$$\mu \partial_y u\big|_{y=h} = \mu^* \partial_{xx} u_s. \tag{4}$$

Substituting (3) into both (2) (evaluated at $y = h(x)$) and (4), and introducing the dimensionless variables $H = h/h_0$, $U = u_s/u_0$, and $X = x/\ell$, leads to

$$H''' = \frac{12}{H^3} - \frac{6 + 6U}{H^2}, \tag{5a}$$

$$\beta\, U'' = -\frac{6}{H^2} + \frac{2 + 4U}{H}, \tag{5b}$$

where a prime denotes the X-derivative and ℓ has been set to ℓ_{Ca} such that $\beta = Bq\,Ca^{2/3}\,\ell_c/h_0$ is the sole independent parameter, and $Bq = \mu*/(\mu\ell_c)$ is the Boussinesq number. The system (5) is solved with the following boundary conditions: $H, U \to 1$ and $H', H'', U' \to 0$ as $X \to \infty$. Furthermore, the curvature of the film profile must match with the curvature of the static meniscus near the bath, which yields the requirement $\partial_{xx} h = \sqrt{2}/\ell_c$ as $x \to -\infty$, or

$$\frac{h_0}{\ell_c} = \frac{H''(-\infty)}{\sqrt{2}}\,Ca^{2/3}. \tag{6}$$

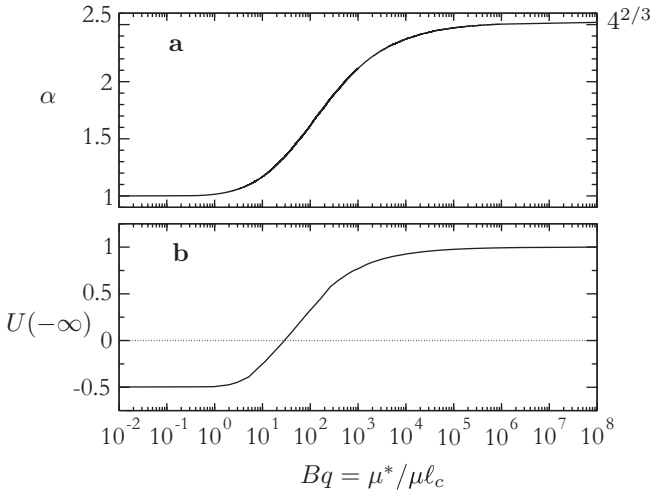

Fig. 2: Effect of surface viscosity $\mu*$ on the thickening factor α and on the matching velocity $U(-\infty)$, as calculated from the model (5).

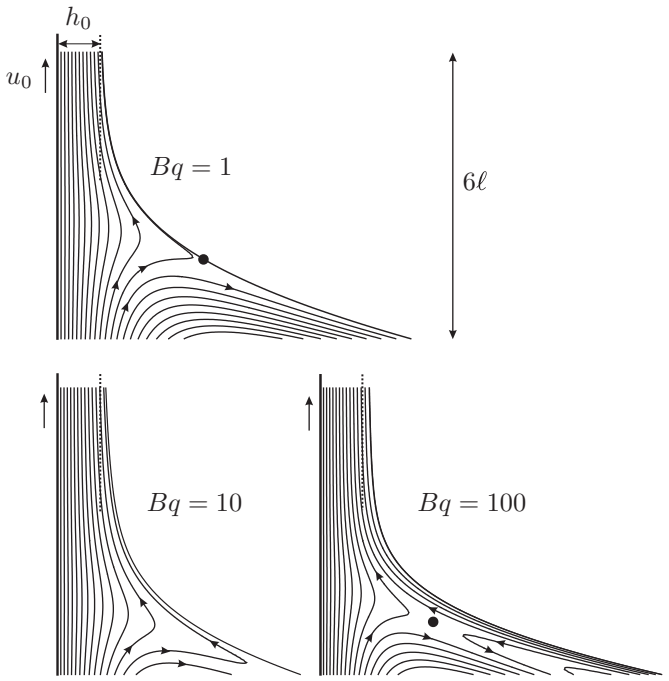

Fig. 3: Streamlines for various Boussinesq numbers Bq. In each plot, the vertical length is $6\ell = 6h_0/Ca^{1/3}$ and the dotted line shows the position of h_0. Dots indicate stagnation points.

Using (6), we find $Bq = \beta\, H''(-\infty)/\sqrt{2}$, which is thus determined *a posteriori* from the solution (β being an input of the calculation and $H''(-\infty)$ being an output).

In the limit of $\beta \to 0$, (5b) gives $U|_{\beta\to 0} = (3-H)/2H$, which substituted into (5a) yields the familiar LLD equation: $H^3 H''' = 3\,(1-H)$. The solution to this equation gives $H''(-\infty) = 1.3376$ such that (6) leads to (1) with $\alpha = 1$. Moreover, as X approaches the static meniscus, $H \gg 1$ such that $U(-\infty) = -1/2$. Notice that the thickening factor for finite β has the form $\alpha = H''(-\infty)/1.3376$, and does not depend on Ca at constant Bq.

In the limit of $\beta \to \infty$, solving (5b) with the boundary conditions for U yields $U|_{\beta\to\infty} = 1$, which substituted into (5a) gives: $H^3 H''' = 12\,(1-H)$, the solution of which leads to (1) with $\alpha = 4^{2/3}$. In this limit, the interface moves at the same speed as the substrate. It is not surprising that α is identical for the cases of an "infinite" surface viscosity and an "infinite" surface elasticity or Marangoni effect (see, *e.g.*, [9,10]), which renders in both cases the surface immobile (relative to the moving plate). Finally, since for the above limits, the matching velocity is constant, we also require $U(-\infty)$ to be constant for any finite value of β, *i.e.* $-\frac{1}{2} \leqslant \beta \leqslant 1$, so as to ensure continuity of the branch of solutions.

Numerical solutions. We solve (5) for finite values of β and scrutinize the transition between the two limits mentioned above. Solutions to (5) were found using a shooting technique (see details in the Appendix A) that ensures both a constant curvature $H''(X)$ and a constant surface velocity $U(X)$ for $X \to -\infty$. Results are shown in fig. 2. Figure 2(a) shows that the thickening factor increases smoothly from 1 to $4^{2/3}$ as Bq increases, demonstrating the possibility of thickening due to pure surface viscosity effects. The best fit we found in the transition region is $\alpha \propto Bq^{1/7}$ though it is only empirical. We also give in the Appendix B a nonlinear fit of the curve α *vs.* Bq. Figure 2(b) shows the surface velocity $U(-\infty)$, which varies monotonically from $-\frac{1}{2}$ to 1 as Bq is increased. We then observe that for $Bq > 25$, $U(-\infty)$ becomes positive, indicating the absence of a stagnation point at the interface, in contrast to the pure LLD limit. We find that $U(-\infty) = 0$ corresponds to $\alpha \approx 1.3$, which differs significantly from the value $\alpha = 2^{2/3} \approx 1.59$ found in the case of pure surface elasticity [11,12].

To understand the role of surface viscosity in the flow behavior, we plot in fig. 3 the streamlines as reconstructed from the stream function defined by $\psi(x,y) = \int u(x,y)\,\mathrm{d}y$. The plot for $Bq = 1$ is comparable to the LLD situation for pure liquids, which includes the presence of a stagnation point at the interface. As the Boussinesq number increases, the stagnation point is displaced downwards (outside the plot area for $Bq = 10$) and eventually disappears from the interface for $Bq > 25$ as found in fig. 2(b). Instead, for $Bq > 25$, the stagnation point moves into the interior of the fluid and is displaced upwards for increasing Bq, as illustrated for $Bq = 100$. This behavior is qualitatively similar to the flow in the case of a pure elastic surface [12], even though the origin of the interfacial stress is different.

Applicability conditions. As conjectured in the introduction, the interface should essentially be viscous beyond the dynamical transition of thickening, *i.e.* no Marangoni effects are expected in the region of "large" capillary numbers. However, the present lubrication model (5) relies on the assumption that gravity is negligible, which is satisfied only for "small" capillary numbers, namely $Ca^{1/3} \ll 1$

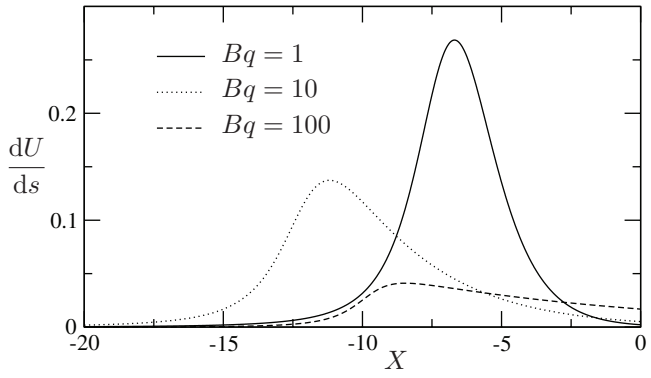

Fig. 4: Rate of stretching of a surface material element along the X-coordinate for various Bq.

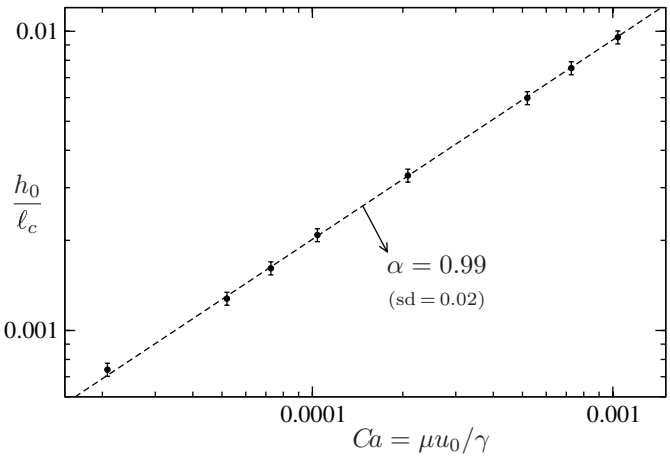

Fig. 5: Experimental results for silicon oil (Si47v20) with no surfactant. The dashed line is a (2/3)-power law corresponding to the mean value of the thickening factor α, with "sd" the standard deviation. Error on Ca values is smaller than the size of the symbols.

assuming $h_0 \approx \ell_c\, Ca^{2/3}$. The region of applicability of the present model is thus restricted to a narrow range of Ca, which only exists at high surfactant concentrations so as to ensure complete surface remobilization and allow neglect of surface elasticity. This regime requires two conditions to be satisfied. First, surfactants should have time to be adsorbed at the interface, and second they should be available in sufficient quantity adjacent to the interface.

The first condition implies that when new interface is generated by stretching on a time scale $\tau_s = \ell/u_0$, surfactants should populate the interface by adsorbing in a time scale $\tau_a \ll \tau_s$. Applying a result obtained in [3] for fiber coating to the case of planar coating, the condition on time scales is

$$\frac{\tau_a}{\tau_s} \approx \frac{\lambda}{\ell_c} \ll 1, \tag{7}$$

where $\lambda = (\gamma_0 - \gamma)\Gamma_0/(kc\mu)$ is a length scale with γ_0 the surface tension of the pure liquid, Γ_0 the saturated surface concentration at equilibrium, and k the intrinsic surfactant adsorption speed. The ratio λ/ℓ_c does not depend on u_0 and is therefore only a property of the surfactant solution. However, since stagnation points also occur at the interface, we cannot dismiss *a priori* the possibility of having different time scales for stretching along the length of the film. We report in fig. 4 the rate of stretching of a surface material element defined as $\mathrm{d}U/\mathrm{d}s = U'/\sqrt{1+H'^2}$. We notice that as the value of Bq increases, the maximum of the velocity derivative diminishes. Therefore, the convective transport becomes less important and the adsorption mechanism works even more efficiently to reduce the concentration gradients since $\mathrm{d}U/\mathrm{d}s = 1$ was assumed when setting $\tau_s = \ell/u_0$.

The second condition implies that

$$\sigma = \frac{\Gamma_0}{ch_0} \approx \frac{\Gamma_0}{c\ell_c Ca^{2/3}} \ll 0.01, \tag{8}$$

where we assumed $\Gamma \approx \Gamma_0$ for bulk concentrations much above the cmc. A typical value is $\Gamma_0 = 1\,\text{molecule}/50\,\text{Å}^2 \simeq 3 \times 10^{-6}\,\text{mol/m}^2$ (see, *e.g.*, [13]). Though (8) has been obtained empirically by Quéré and de Ryck [3] for DTAB, we assume this condition to be applicable for the surfactant used in the experiments we next describe, since the molecules are very similar.

Experiments. – Experiments using water solutions of the surfactant dTAB (decyl trimethyl ammonium bromide) have been performed at high concentrations. This surfactant with cmc = 66 mM was chosen for its greater solubility in water than DTAB. The surface tension was measured by the Wilhelmy plate method. The shear viscosity of the liquid was measured by a rheometer (Anton Paar Physica MCR 300) with an embedded double Couette cylindrical system (DG 26.7/TEZ 150 P-C) [14]. The substrate used was a silicon wafer. The film thickness was measured using a multi-wavelength light reflected on the film and analyzed with a spectrometer (Ocean Optics). The error on the thickness measurement was evaluated at 5%, and is reported by the error bars in the subsequent plots. We validated the measurement technique with a pure liquid by comparing the mean value of the thickening factor obtained for each thickness measurement. The results are shown in fig. 5, where the dashed line corresponds to the mean value for the thickening factor, $\alpha = 0.99$, which is 1% below the theoretical value, lying in turn within the standard deviation (sd) of 2%. The reason we performed the control experiment with silicon oil and not with water is because water is easily contaminated and it was impossible to keep pure water clean during a complete set of measurements. Indeed, it is known that a very small amount of impurities at a water surface can induce a strong Marangoni effect [15]. However, as long as surfactant ($c >$ cmc) is added to water, these difficulties disappear, as the impurities (mainly fatty substances) get dissolved in the micelles and the monolayer remains only populated by added surfactants [16].

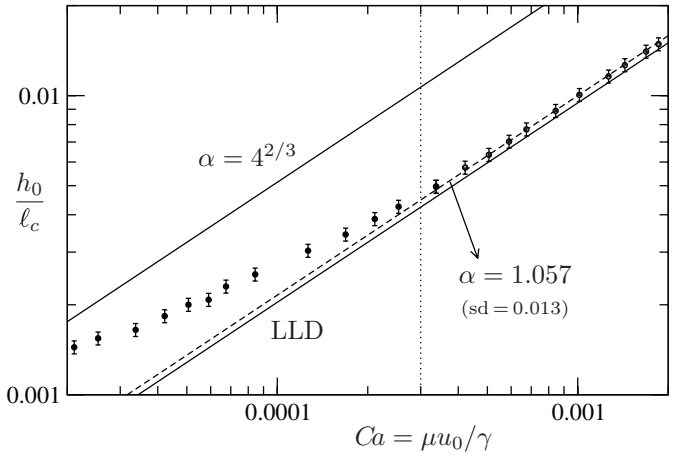

Fig. 6: Experimental results for dTAB with $c = 15\,\mathrm{cmc}$. Solid lines are the bounds for the thickening factor. The dashed line is a (2/3)-power law corresponding to the mean value of α beyond the "dynamical transition of thickening" (dotted line).

Figure 6 shows the measured variation of the film thickness with the capillary number for $c = 15\,\mathrm{cmc}$. The dotted line separates the dynamical transition of thickening on the left, to a zone of constant thickening on the right. Though large thickening is usually attributed to surface elasticity, the dynamical transition shows a decrease of the thickening with *Ca*. As mentioned in the introduction, this phenomenon is due to the surface remobilization caused by the increase of the film thickness, which increases the number of surfactants available to replenish the interface (as quantified by the parameter σ). Having also performed experiments for smaller concentration (not shown), we observed a shift of the dynamic transition of thickening toward smaller *Ca* values for increasing the concentration. Consequently, the experiment for high concentration ($c = 15\,\mathrm{cmc}$) allowed us to put in evidence a zone of constant thickening for almost a decade in *Ca* beyond the dynamical transition.

The mean value of the thickening factors for the experimental points lying on the right of the dotted line in fig. 6 gives $\alpha \approx 1.06$, with a standard deviation of about 1%. Though small, this 6% thickening exceeds the errors associated with our experimental method (1% for pure liquid). Such a result thus demonstrates the existence of a thickening effect induced by the presence of surfactant in a regime where no concentration gradient exists, *i.e.* for which conditions (7) and (8) are satisfied. To evaluate the intrinsic adsorption speed k, and considering the worst case, we added to the diffusion process (*i.e.* $D/a \approx 0.1\,\mathrm{m/s}$, with D the diffusion coefficient and a the molecular size) a small electrostatic barrier of $V = 100\,\mathrm{mV}$, common for large surfactant concentrations, which gives $k = (D/a)e^{-V/k_bT} \approx 10^{-3}\,\mathrm{m/s}$, with $k_bT \approx 25\,\mathrm{mV}$. Taking $\gamma_0 = 0.072\,\mathrm{N/m}$, $\gamma = 0.04\,\mathrm{N/m}$, $\mu = 0.00335\,\mathrm{Pa\,s}$ and $\rho = 1000\,\mathrm{kg/m^3}$, leads, for $c = 990\,\mathrm{mM}$ and $Ca = 10^{-3}$, to $\tau_a/\tau_s \approx 10^{-2}$ and $\sigma \approx 10^{-4}$, which indeed fully satisfies conditions (7) and (8).

We can therefore state that the constant thickening observed in fig. 6 should essentially be induced by surface viscosity effects. We then use our model to assess the value of surface viscosity corresponding to $\alpha = 1.06$, and from fig. 2(a), we get the corresponding Boussinesq number $Bq \approx 3$. Using $\ell_c \approx 2\,\mathrm{mm}$, we finally obtain $\mu* \approx 2 \times 10^{-5}\,\mathrm{Pa\,s\,m}$, which is consistent with typical values reported in the literature for ionic surfactants (see, *e.g.*, [17,18]). One should mention that this small value was at the limit of resolution of the surface rheometer (Anton Paar Physica MCR 301 with an embedded interfacial rheology system) available to us at the time of this study, which did not permit a direct measurement of the surface viscosity.

It is known that surface viscosity has two contributions, namely "intrinsic" viscosity associated with the shear between surfactants at the interface, and "exchange" viscosity arising from the energy dissipation associated with the exchange of surfactants between the surface and the sublayer (see, *e.g.*, [7]). Though exchange viscosity is usually much higher than intrinsic viscosity at low c [19], it inherently vanishes with surface elasticity at large c (see, *e.g.*, [20]) such that intrinsic surface viscosity alone should be responsible for thickening in the parameter range that satisfies the conditions (7) and (8) for complete surface remobilization.

Conclusions. – We conclude that the constant thickening observed in the dip-coating process at large *Ca* values with surfactants of high solubility and at high concentration can be rationalized entirely by the effect of intrinsic surface viscosity. Moreover, based on our findings, we anticipate that the large constant thickening observed at small *Ca* values (see fig. 6) should not only be due to surface elasticity, as generally proposed in the literature, but to cooperative effects of both surface elasticity and surface viscosity, with an even bigger influence of the surface viscosity than in the present study due to its "exchange" component. For instance, this argument could be a candidate to resolve the apparent paradox reported by Krechetnikov and Homsy [21] between the strong thickening observed in experiments in contrast with the thinning predicted by their simulations. In any case, it is clear that surface rheology deserves closer study for a better understanding of flows dominated by the presence of fluid-fluid interfaces containing surface-active materials.

* * *

We thank Saint-Gobain Recherche for support of this investigation. BS thanks the Brussels Region for the funding through the program "Brains Back to Brussels".

Appendix A: shooting procedure. – We detail in this appendix the shooting procedure used in the numerical resolution of (5). We first look for approximate solutions in the vicinity of the flat film region, *i.e.* $H, U \to 1$ as $X \to \infty$. Those local solutions are sought in the form $H = 1 + ae^{\lambda X}$ and $U = 1 + be^{\lambda X}$. Substituting those

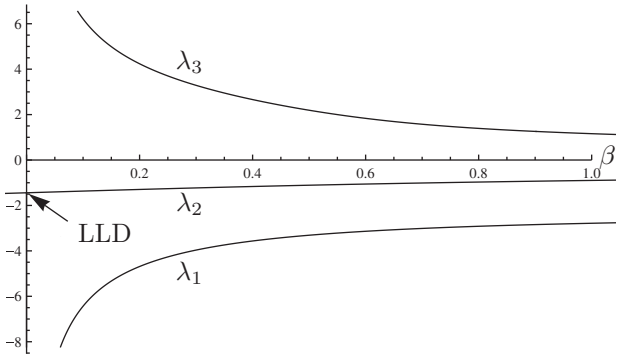

Fig. 7: Real eigenvalues *vs.* β obtained from (A.1). Note a unique real eigenvalue is obtained in the LLD limit for $\beta \to 0$.

expressions into (5) and linearizing with respect to the small amplitudes a and b, we find the characteristic equation for the eigenvalue λ,

$$4 - \beta\lambda^2 - \frac{36}{12+\lambda^3} = 0. \qquad \text{(A.1)}$$

Among the five roots of this equation, three are real (one positive and two negative) and plotted in fig. 7 as a function of β. The local solution should therefore be a linear combination of the solutions corresponding to the negative eigenvalues, noted λ_1 and λ_2. We can thus write $H = 1 + a_1 e^{\lambda_1 X} + a_2 e^{\lambda_2 X}$ for the local solution near the flat film region. The amplitudes b_1 and b_2 for the surface velocity U are determined from $b_i = -6a_i/(4 - \beta\lambda_i^2)$. Since solutions are invariant by translation along the X-coordinate, we can fix one of the two amplitudes and use the other as the shooting parameter. We chose in fact to fix the curvature of the solution, taking $X = 0$ as reference, such that $H''(0) = a_1\lambda_1^2 + a_2\lambda_2^2$. For all calculations, we have taken $H''(0) = 10^{-3}$. The rest of the procedure thus consists in shooting from $X = 0$ toward negative values by progressively extending the domain and adjusting the single shooting parameter such that H'' and U eventually tend to constants, namely $H''(-\infty)$ and $U(-\infty)$. It was found that a domain of 15ℓ was large enough to satisfy these criteria for any value of Bq.

Appendix B: nonlinear fit of α vs. Bq. – We propose here a nonlinear fit of the curve plotted in fig. 2(a),

$$\alpha \cong \frac{1}{2} + 2^{1/3} + \left(2^{1/3} - \frac{1}{2}\right) \tanh\left[6.40 - 8.27 Bq^{-0.049}\right],$$

which can be inverted to get a rough estimate of the value of the Boussinesq number Bq, hence the surface viscosity $\mu*$, for a given thickening factor α.

REFERENCES

[1] Scriven L. E. and Sternling C. V., *Nature*, **187** (1960) 186.
[2] Park C.-W., *J. Colloid Interface Sci.*, **146** (1991) 382.
[3] Quéré D. and de Ryck A., *Ann. Phys. (Paris)*, **23** (1998) 1.
[4] Stebe K. J., Lin S.-Y. and Maldarelli C., *Phys. Fluids A*, **3** (1991) 3.
[5] Levich V. G., *Physicochemical Hydrodynamics* (Prentice-Hall) 1962.
[6] Sonin A. A., Bonfillon A. and Langevin D., *Phys. Rev. Lett.*, **71** (1993) 2342.
[7] Lucassen-Reynders E. H. and Lucassen J., *Adv. Colloid Interface Sci.*, **2** (1969) 347.
[8] Naire S., Braun R. J. and Snow S. A., *Phys. Fluids*, **13** (2001) 2492.
[9] Shen A. Q., Gleason B., McKinley G. H. and Stone H. A., *Phys. Fluids*, **11** (2002) 4055.
[10] Tiwari N. and Davis J. M., *Phys. Fluids*, **18** (2006) 022102.
[11] Ou Ramdane O. and Quéré D., *Langmuir*, **13** (1997) 2911.
[12] Ramé E., *Phys. Fluids*, **19** (2007) 078102.
[13] Evans D. F. and Wennerstrom H., *The Colloidal Domain: Where Physics, Chemistry, Biology, and Technology Meet*, 2nd edition (John Wiley and Sons) 1994.
[14] Erni P., Fischer P., Windhab E. J., Kusnezov V., Stettin H. and Läuger J., *Rev. Sci. Instrum.*, **74** (1996) 4916.
[15] Ratulowski J. and Chang H.-C., *J. Fluid Mech.*, **303** (1990) 210.
[16] Mysels K. J. and Stafford R. E., *Colloids Surf.*, **51** (1990) 105.
[17] Prud'homme R. K. and Khan S. A., *Foams: Theory, Measurements, and Applications* (CRC Press) 1995.
[18] Stevenson P., *J. Colloid Interface Sci.*, **290** (2005) 603.
[19] Edwards D. A., Brenner H. and Wasan D. T., *Interfacial Transport Processes and Rheology* (Butterworth-Heinemann, Boston) 1991.
[20] Stenvot C. and Langevin D., *Langmuir*, **4** (1988) 1179.
[21] Krechetnikov R. and Homsy G. M., *J. Fluid Mech.*, **559** (2006) 429.